ADVANCED FUNCTIONAL MATERIALS

Supporting Information

for *Adv. Funct. Mater.,* DOI: 10.1002/adfm.202105028

Bioresponsive, Electroactive, and Inkjet-Printable Graphene-Based Inks

Alessandro Silvestri, Alejandro Criado, Fabrizio Poletti, Faxing Wang, Pablo Fanjul-Bolado, María B. González-García, Clara García-Astrain, Luis M. Liz-Marzán, Xinliang Feng, Chiara Zanardi, and Maurizio Prato**

Supporting Information

Bio-responsive, Electroactive and Inkjet-printable Graphene-based Inks

Alessandro Silvestri, Alejandro Criado, Fabrizio Poletti, Faxing Wang, Pablo Fanjul-Bolado, María B. González-García, Clara García-Astrain, Luis M. Liz-Marzán, Xinliang Feng, Chiara Zanardi, Maurizio Prato**

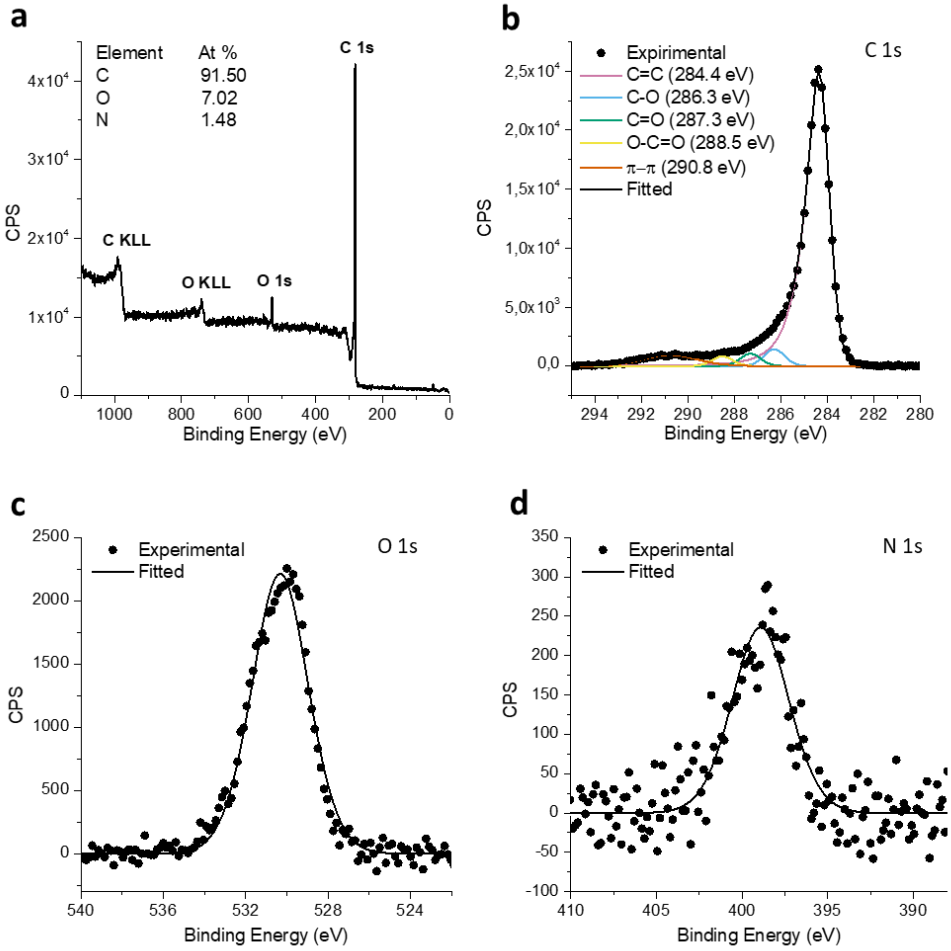

Figure S1. Full XPS characterization of pristine EEG. A**)** XPS survey spectrum. B) High-resolution XPS spectra of the C1s core. C) High-resolution XPS spectra of the O1s core level. D) High-resolution XPS spectra of the N1s core level.

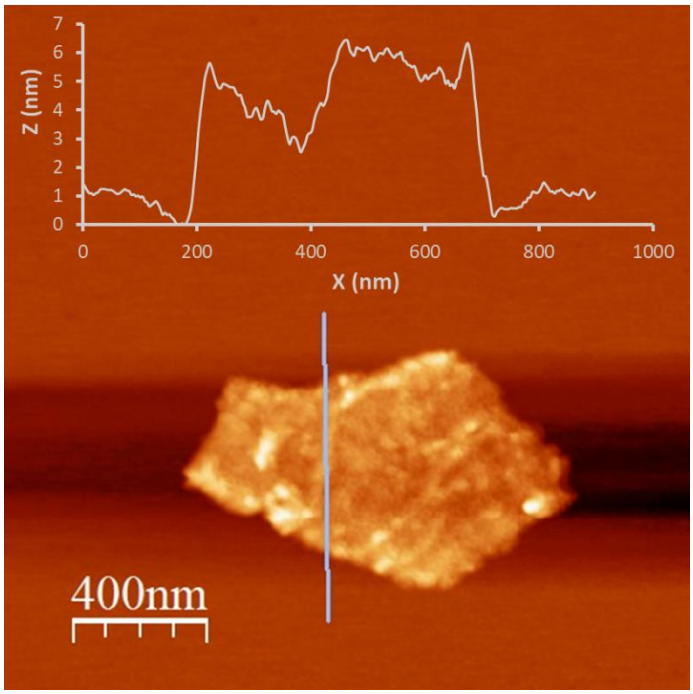

Figure S2. AFM height micrograph of the pristine EEG. Insight: AFM height profile of a graphene flake.

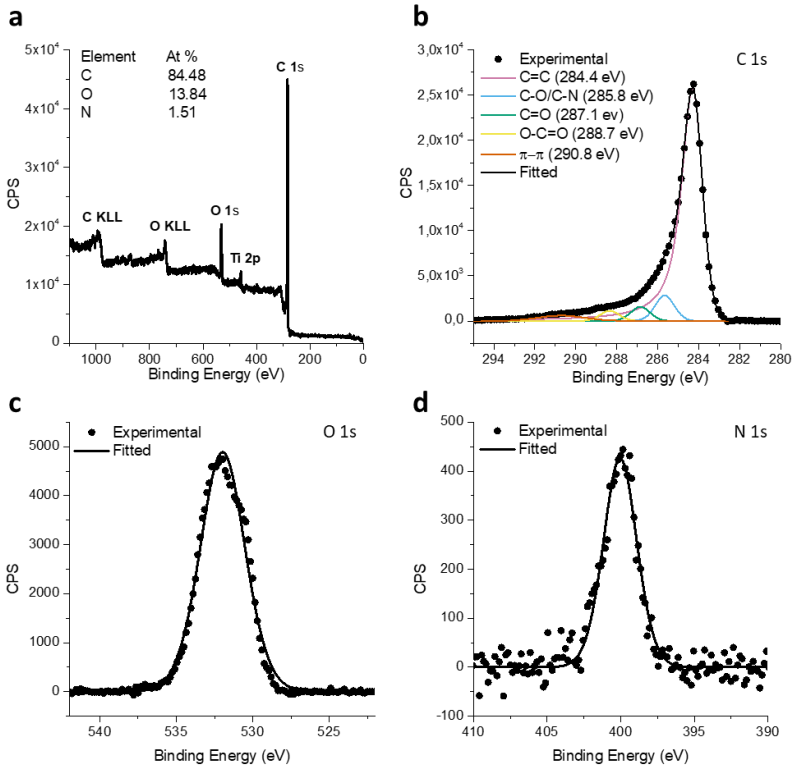

Figure S3. Full XPS characterization of EEG-COOH. A) Low-resolution XPS survey spectrum. B) High-resolution XPS spectra of the C1s core. C) High-resolution XPS spectra of the O1s core. D) High-resolution XPS spectra of the N1s core.

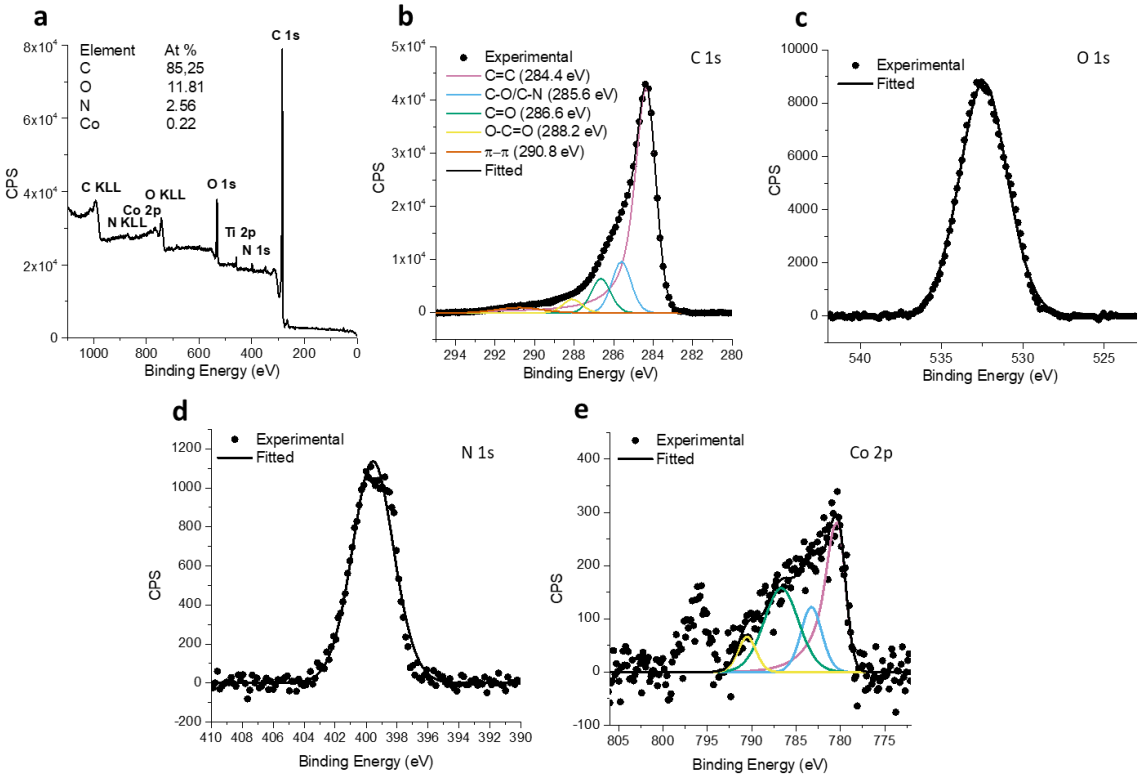

Figure S4. Full XPS characterization of EEG-COOH-CoPC. A) Low-resolution XPS survey spectrum. B) High-resolution XPS spectra of the C1s core level. C) High-resolution XPS spectra of the O1s core level. D) High-resolution XPS spectra of the N1s core level. E) High-resolution XPS spectra of the Co2p core level.

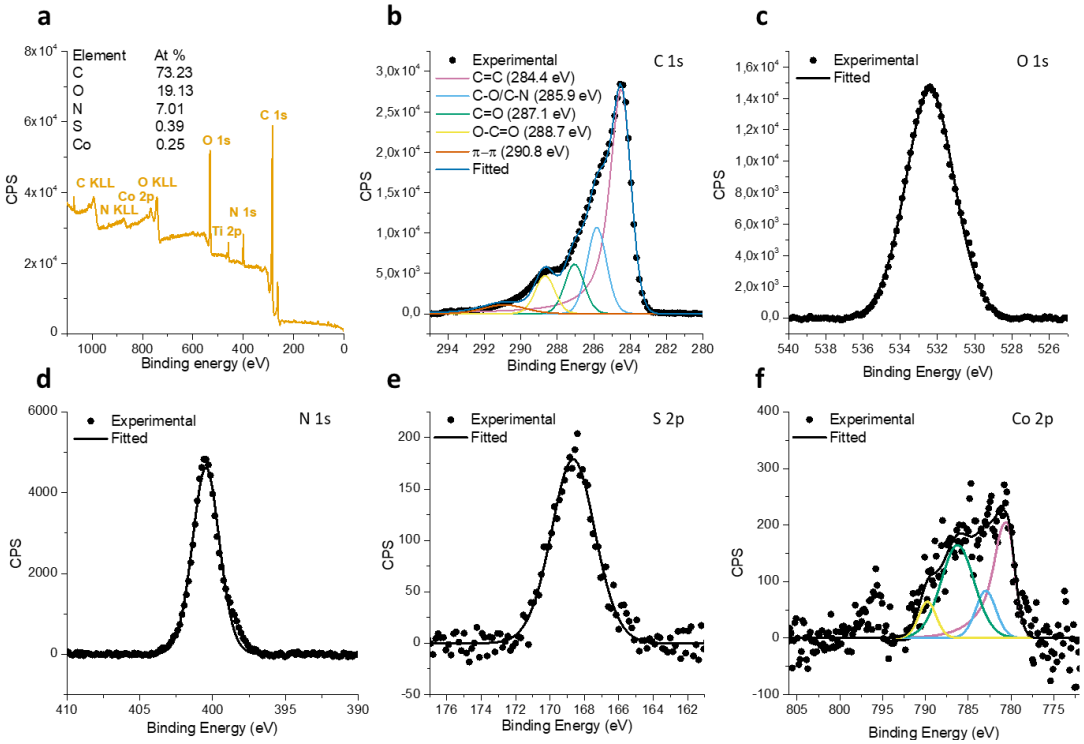

Figure S5. Full XPS characterization of EEG-GOx-CoPC. A) Low-resolution XPS survey spectrum. B) High-resolution XPS spectra of the C1s core level. C) High-resolution XPS spectra of the O1s core level. D) High-resolution XPS spectra of the N1s core level. E) High-resolution XPS spectra of the S2p core level. F) High-resolution XPS spectra of the Co2p core level.

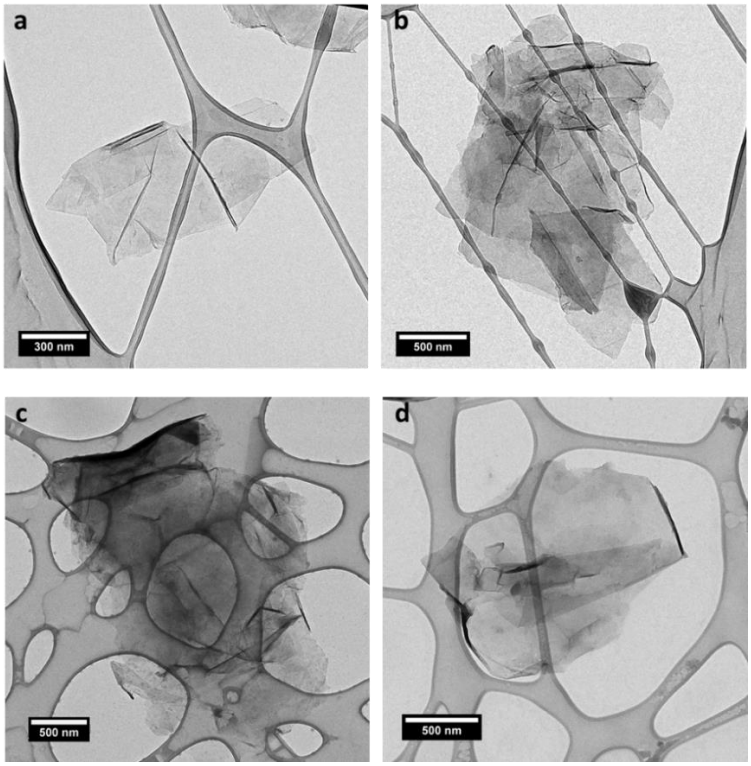

Figure S6. TEM micrographs of A) EEG B) EEG-COOH C) EEG-COOH-CoPC D) EEG-GOx-CoPC

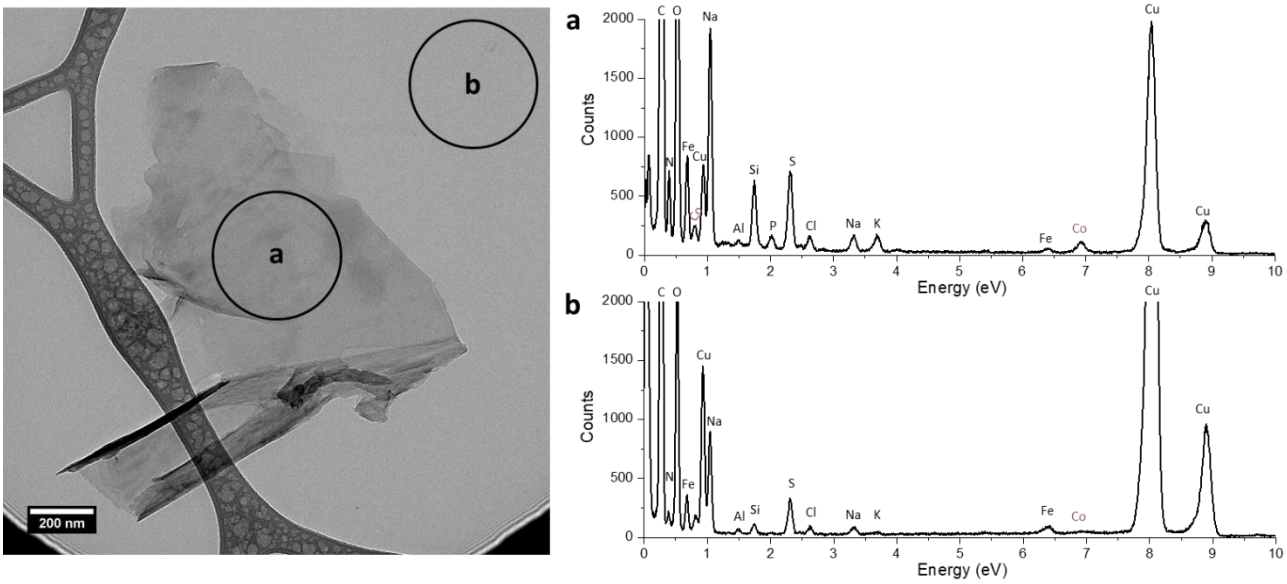

Figure S7. TEM-EDX analysis of EEG-GOx-CoPC. On the left the TEM micrograph of the graphene flake with highlighted the two regions of the analysis. On the right the EDX spectra of region *a* and *b*. It is possible to notice that Co signal is localized on the graphene flake, and absent in the background, proving CoPC absorption.

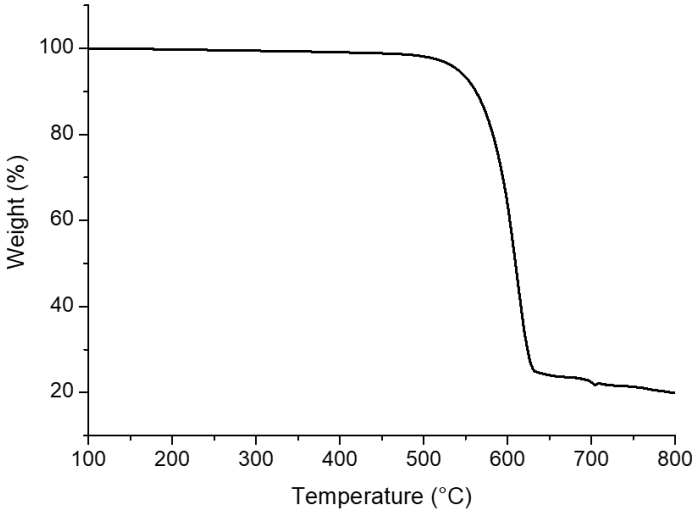

Figure S8. TGA of CoPC under N_2. Cobalt phthalocyanine starts to degrade at 500 °C under N_2 environment.

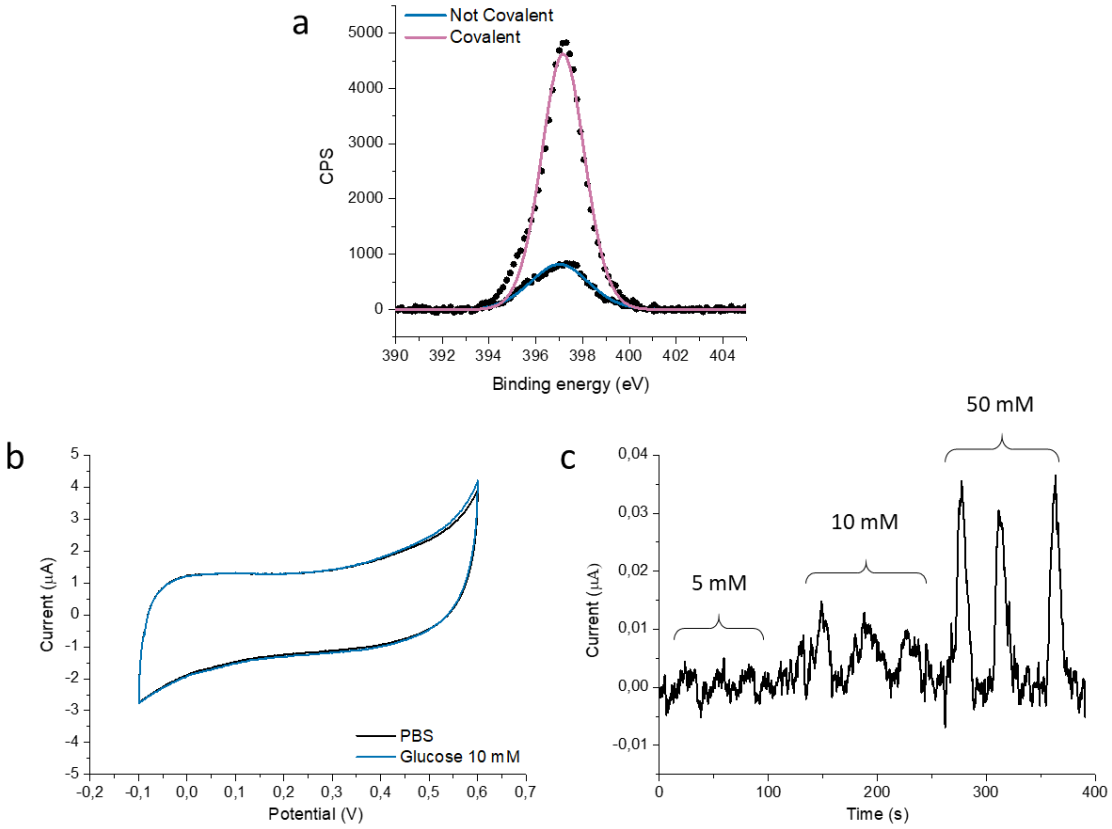

Figure S9. Covalent anchoring of the enzyme is required and effective to reach high functionalization degrees and intense electrochemical responses. A control experiment has been performed incubating graphene with GOx without coupling reagents (EDC, NHS). The functionalization degree, evaluated by mean of XPS N content (A), resulted to be lower by far compared to the covalently bounded system. As result of the low amount of GOx adsorbed over graphene the currents generated from the final ink in CV (B) and FIA (C) are extremely low. Such experiment proves that the covalent conjugation is effective, and the enzyme is not simply adsorbed on the graphene, because physical adsorption does not allow to reach the functionalization degree experimented after amidation.

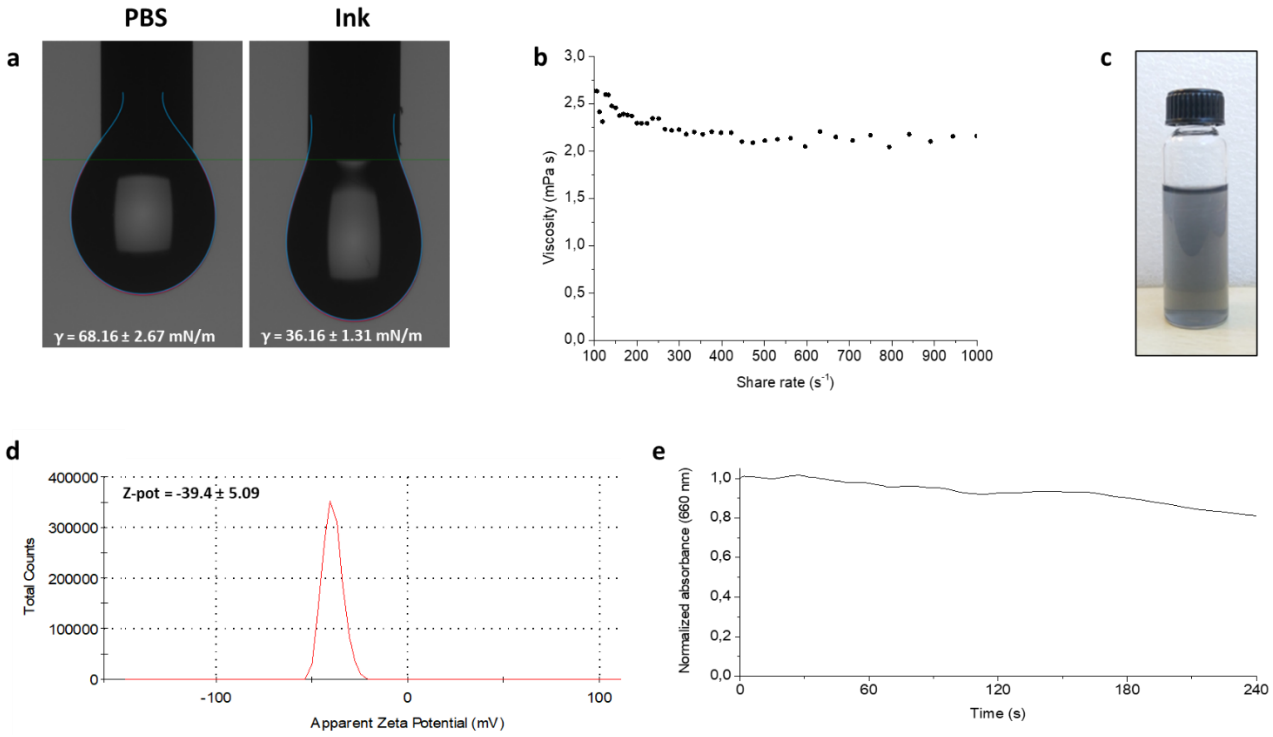

Figure S10. Characterization of the ink formulation. A) Surface tension (γ) of EEG-GOx-CoPC in PBS and of the EEG-GOx-CoPC ink (1 mg ml^{-1}) measured by pendant drop analysis B) Dynamic viscosity profile of the ink (1 mg ml^{-1}). The viscosity extrapolated at high share rates is equal to 2.14 mPa s C) Picture showing the EEG-GOx-CoPC ink at a concentration of 0.25 mg ml^{-1} D) ζ-pot of the EEG-GOx-CoPC ink at a concentration of 0.25 mg ml^{-1} E) Sedimentation rate of EEG-GOx-CoPC (0.25 mg ml^{-1}) ink, evaluated through the variation of the absorption value at 660 nm over the time.

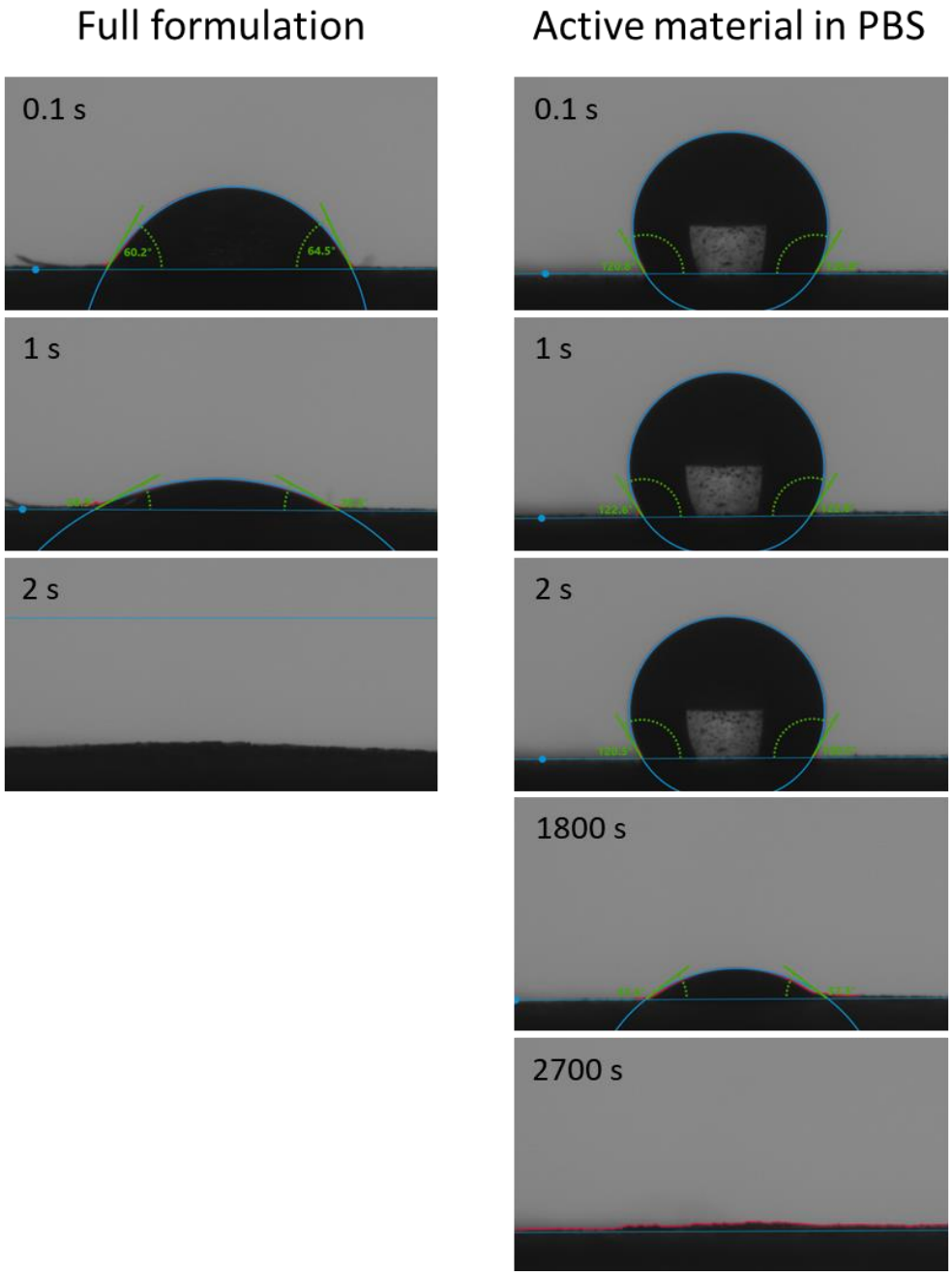

Figure S11. Contact angle measurements at different time points during drying of the ink with the full formulation and with the active material in PBS (without cosolvents), on partially hydrophobized paper (drop volume 2.0 µL). The ink formulation effectively reduces the surface tension of water in contact with the paper, reducing the contact angle from 120.8° to 62.35° (at timepoint 0.1 s). Furthermore, the ink formulation improves the wettability of the ink allowing complete adsorption within less than 2 seconds, while the active material in PBS took more than 30 minutes to dry completely.

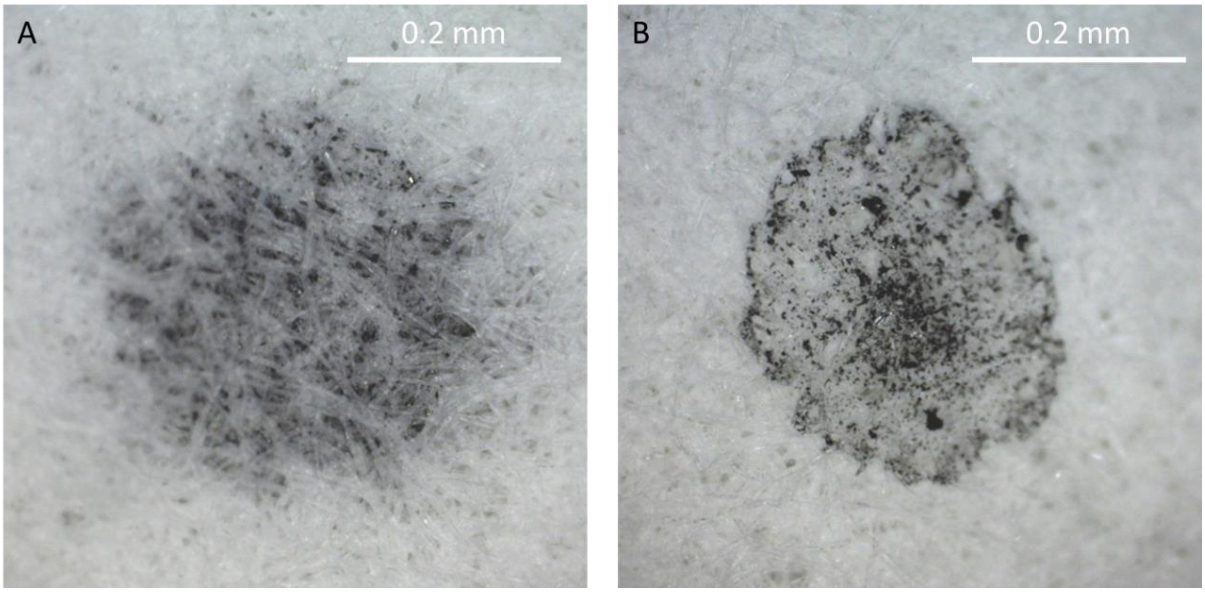

Figure S12. Optical micrographs of the material deposited on partially hydrophobic paper, upon drying a 2.0 μL drop of the ink (A) and of the active material in PBS (B). The ink formulation improves the homogeneous distribution of the material in the spot and hinders coffee-ring formation

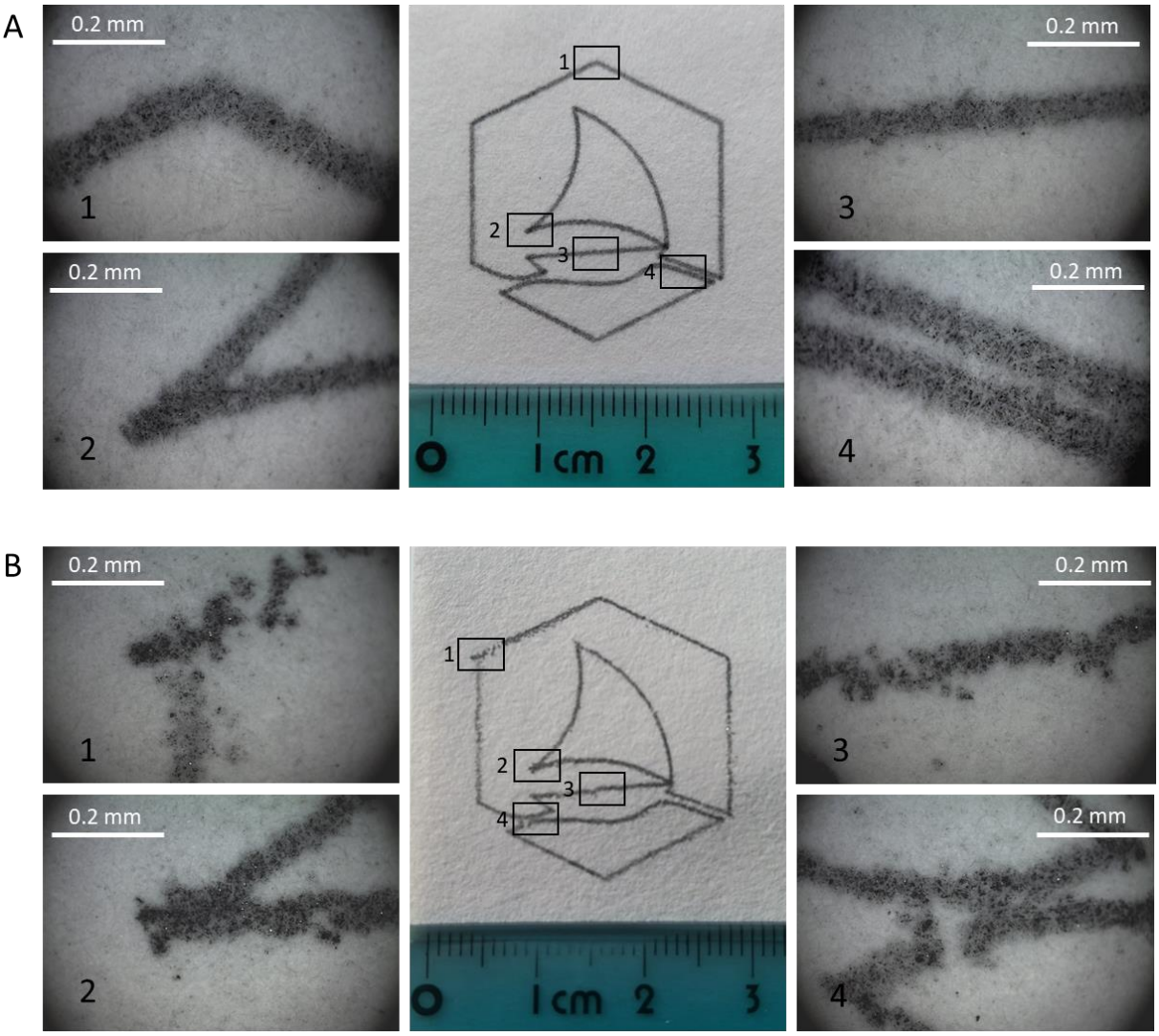

Figure S13. Pictures and optical micrographs of the Graphene Flagship logo, obtained by inkjet printing with the full ink formulation (A) and with the active material in PBS (B). The optical micrographs show details of the logo, highlighting the differences in homogeneity, continuity, and precision of the line between the ink and the control.

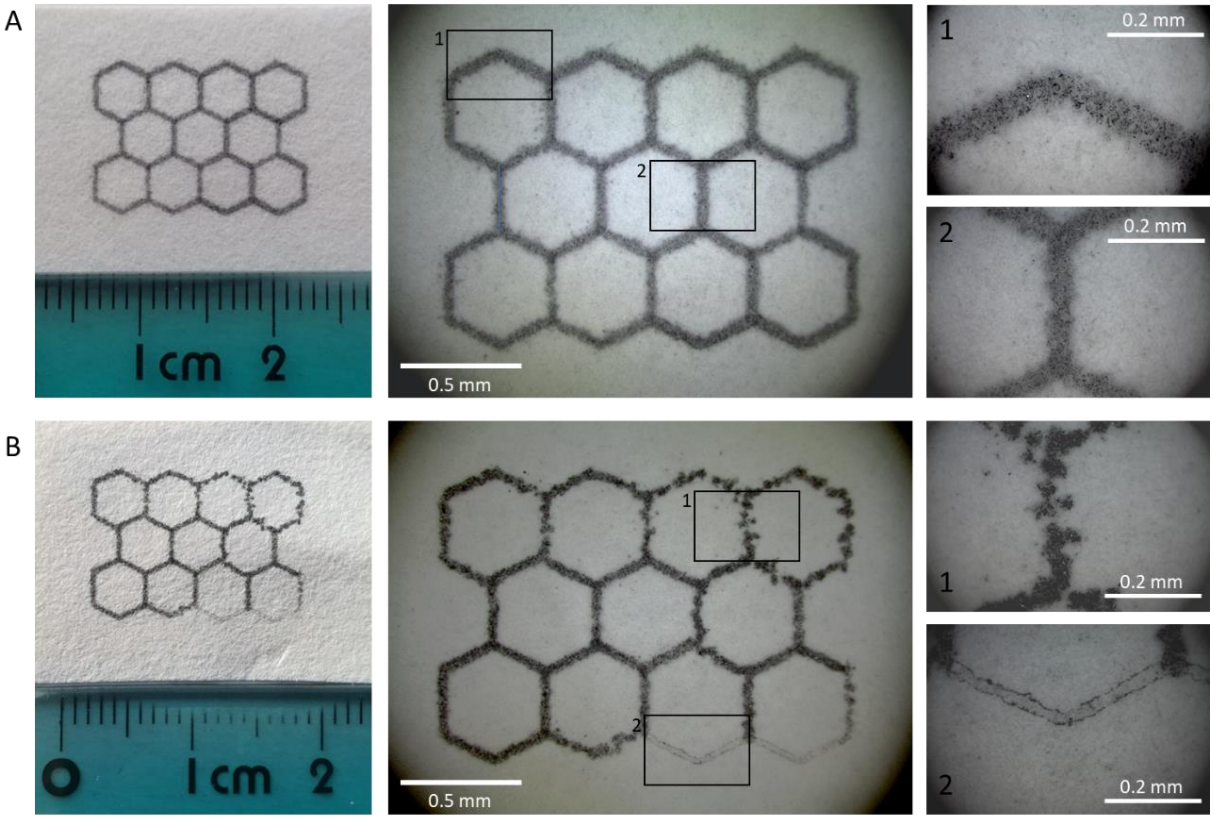

Figure S14. Pictures and optical micrographs of a graphene-like honeycomb structure obtained by inkjet printing with the full ink formulation (A) and with the active material in PBS (B). The optical micrographs show details of the structure, highlighting the differences in homogeneity, continuity, and precision of the line between the ink and the control.

Performace of glucose-responsive ink	
Linear Range (mM)	0.1-10.0
Sensitivity (µA cm^{-2} mM^{-1})	0.261
Reproducibility (RSD%)	3.60
Repeatability (RSD%)	8.85
LOD (µM)	8

Table S1. Table summarzing the analytical performance of the EEG-GOx-CoPC ink

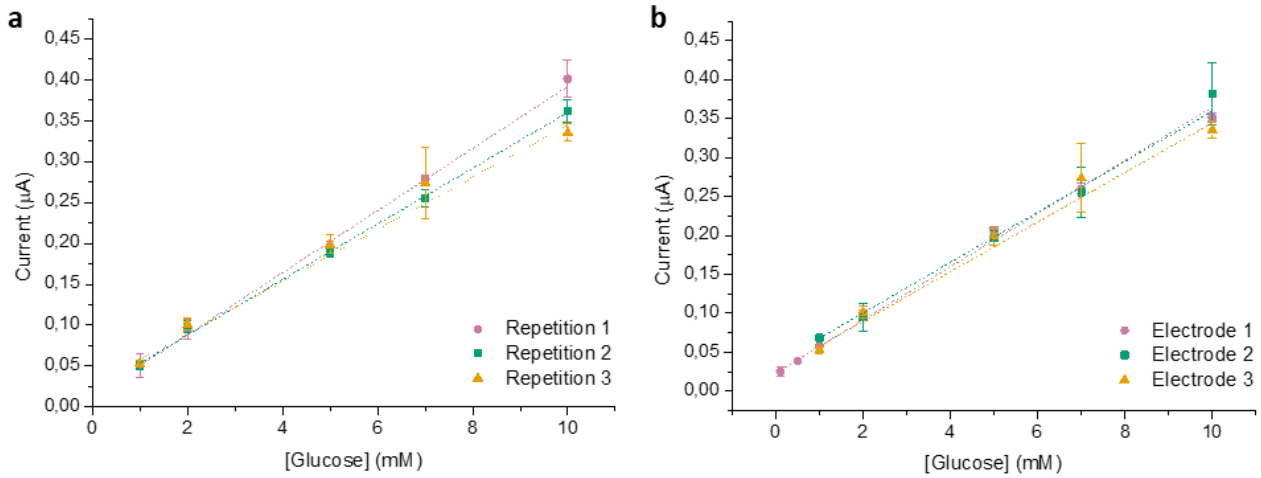

Figure S15. Repeatability and reproducibility of C-SPE electrodes modified with EEG-GOx-CoPC. A) Calibration lines obtained from three consecutive FIAs on the same C-SPE electrode modified with the ink. The RSD% calculated among the three slopes of the linear calibrations was of 8.85 %. Error bars represent the standard deviation among three injections in the same analysis. B) Calibration lines obtained from three different electrodes. The RSD% calculated among the three slopes of the linear calibrations was of 3.60 %. Error bars represent the standard deviation among three injections in the same analysis.

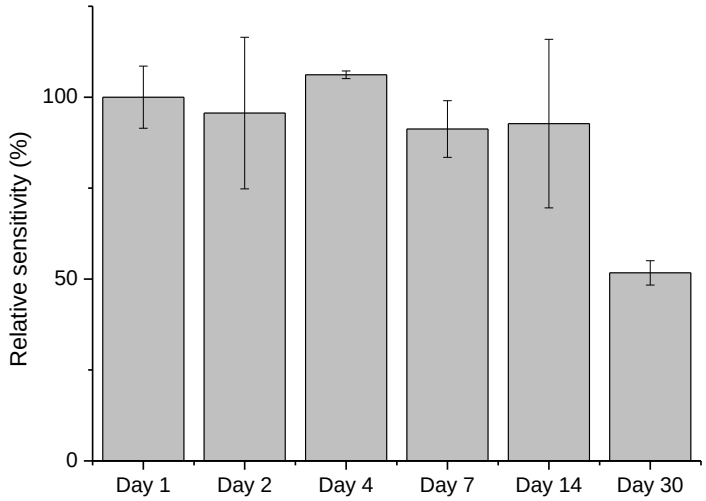

Figure S16. Relative sensitivity of the EEG-GOx-CoPC ink versus time. For every time point, three FIA measurements were performed on different electrodes. The sensitivity of each electrode was evaluated in the linearity range (0.5-10.0 mM). The reported values are the average among the sensitivity of the three electrodes.

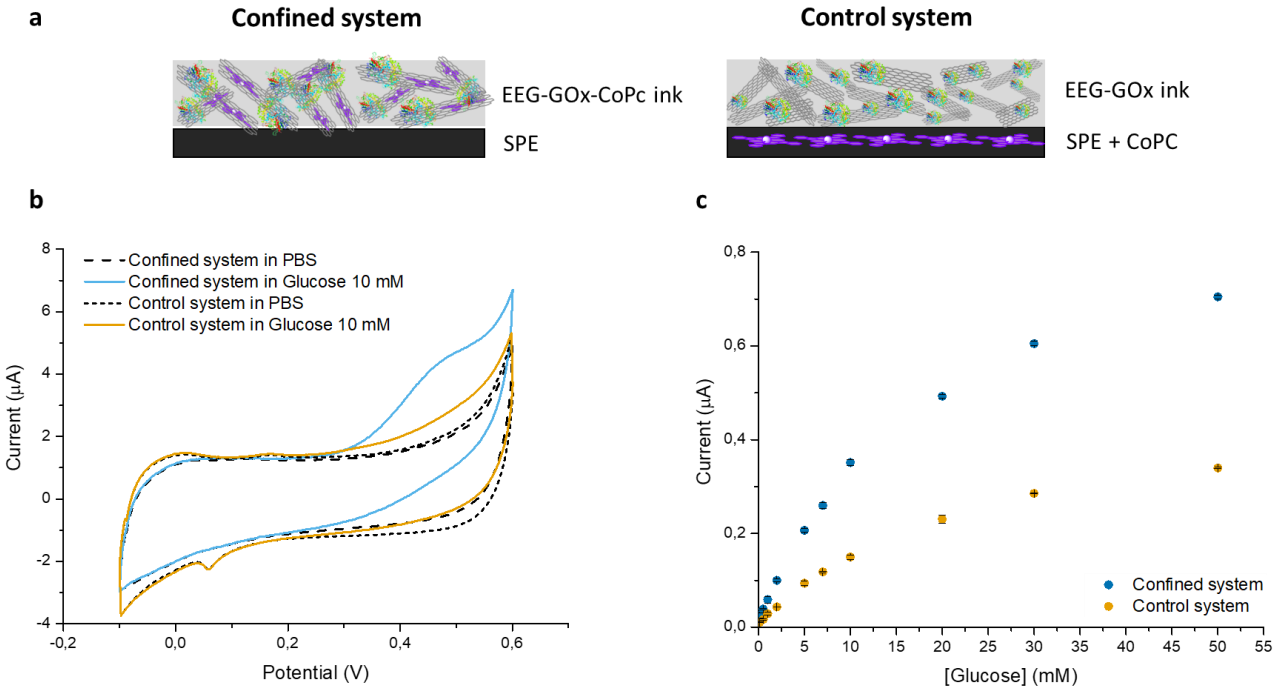

Figure S17. Effect of nano-confinement on the electrochemical properties of the ink. A) Schematic representation of the confined system (where EEG-GOx-CoPC ink was deposited over a SPE electrode) and the control system (where CoPC was deposited on the SPE electrode and EEG-GOx ink was deposited on top of that). B) CV responses of the confined and control systems in PBS in absence and in presence of 10 mM glucose (scan rate 20 mV s^{-1}). C) Plotting of the current intensities registered in FIA versus the glucose concentration. Error bars represent the standard deviation among three injections in the same analysis.

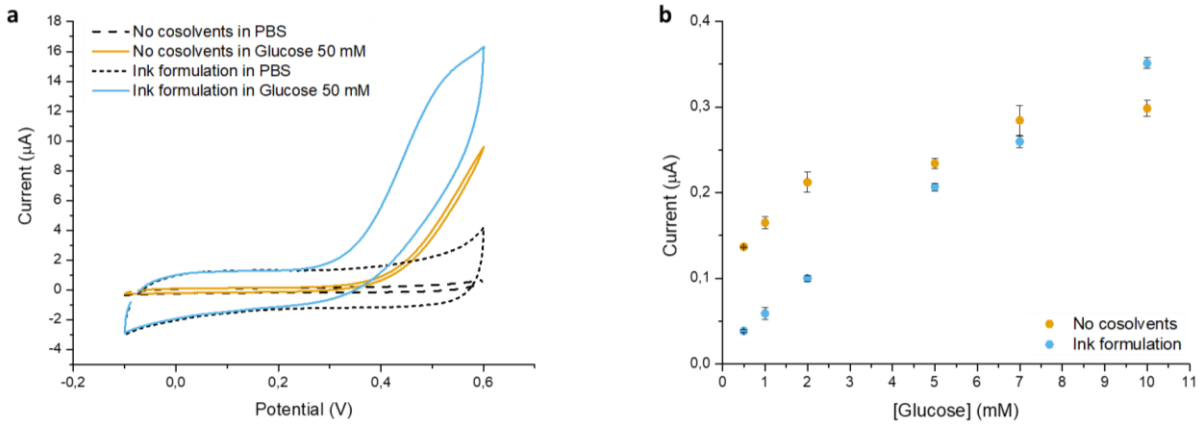

c	Full formulation	Active material (without cosolvents)
Linear Range (mM)	0.1-10.0	0.1-2
Sensitivity (µA cm^{-2} mM^{-1})	0.261	0.414
Reproducibility (RSD%)	3.60	5.96
LOD (µM)	8	2

Figure S18. Comparison between the electrochemical performance of the ink (full formulation) and the active material (without *t*-BuOH and propylene glycol). a) CV responses of the ink with and without cosolvents in PBS in absence and in presence of 50 mM glucose (scan rate 20 mV s^{-1}). b) Plot of the current intensities registered in FIA (E=+0.4 V) versus glucose concentration. Error bars represent the standard deviation among three injections in the same analysis. c) Table summarizing the electrochemical performance of the ink (full formulation) and of the active material (without cosolvents).

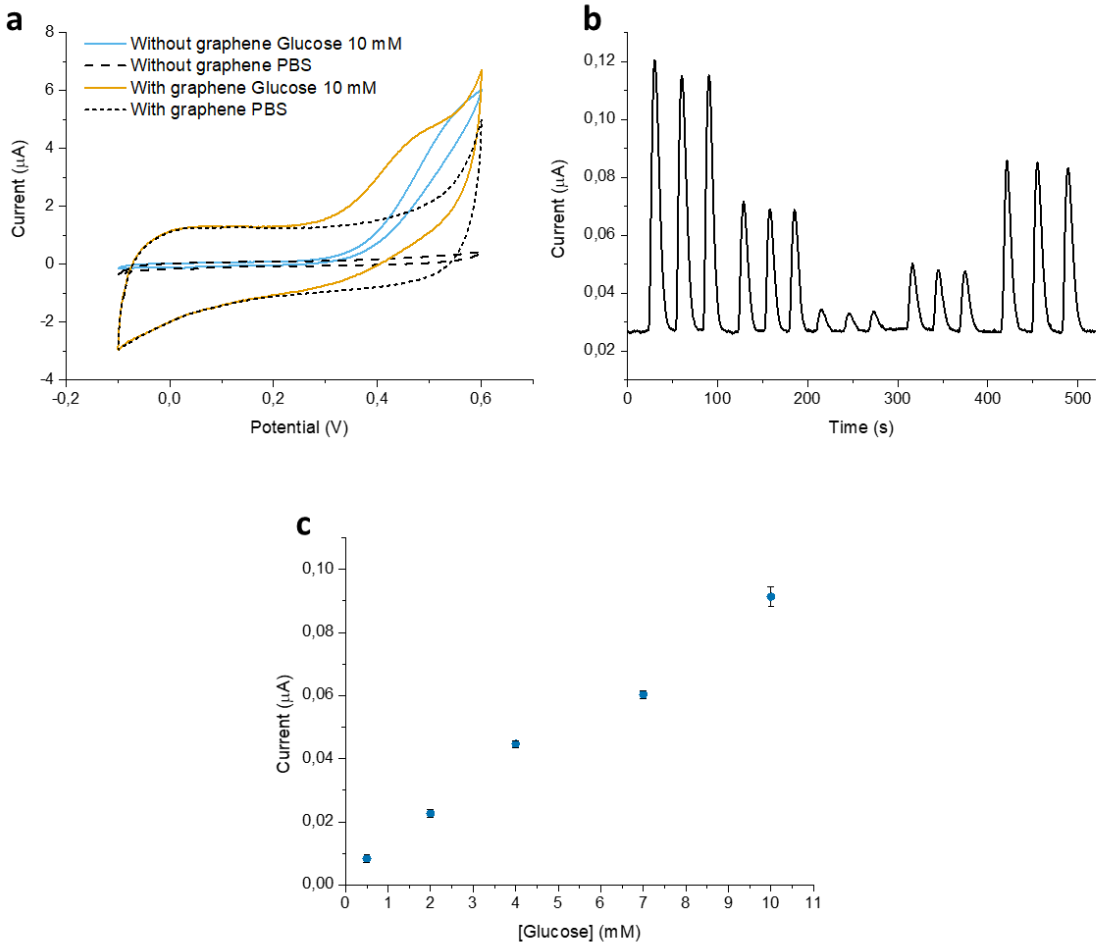

Figure S19. Effect of the presence of graphene on the ink response. A) CV responses of the ink with and without graphene in PBS in absence and in presence of 10 mM glucose (scan rate 20 mV s^{-1}). B) Representative FIA response of the ink without graphene deposited on the SPE. Five glucose concentration levels were tested: 0.5, 2.0, 4.0, 7.0, 10.0 mM. C) O Plot of the current intensities registered in FIA versus the glucose concentration. Error bars represent the standard deviation among three injections in the same analysis. The resulting sensitivity is equal to 0.067 µA cm^{-2} mM^{-1}.

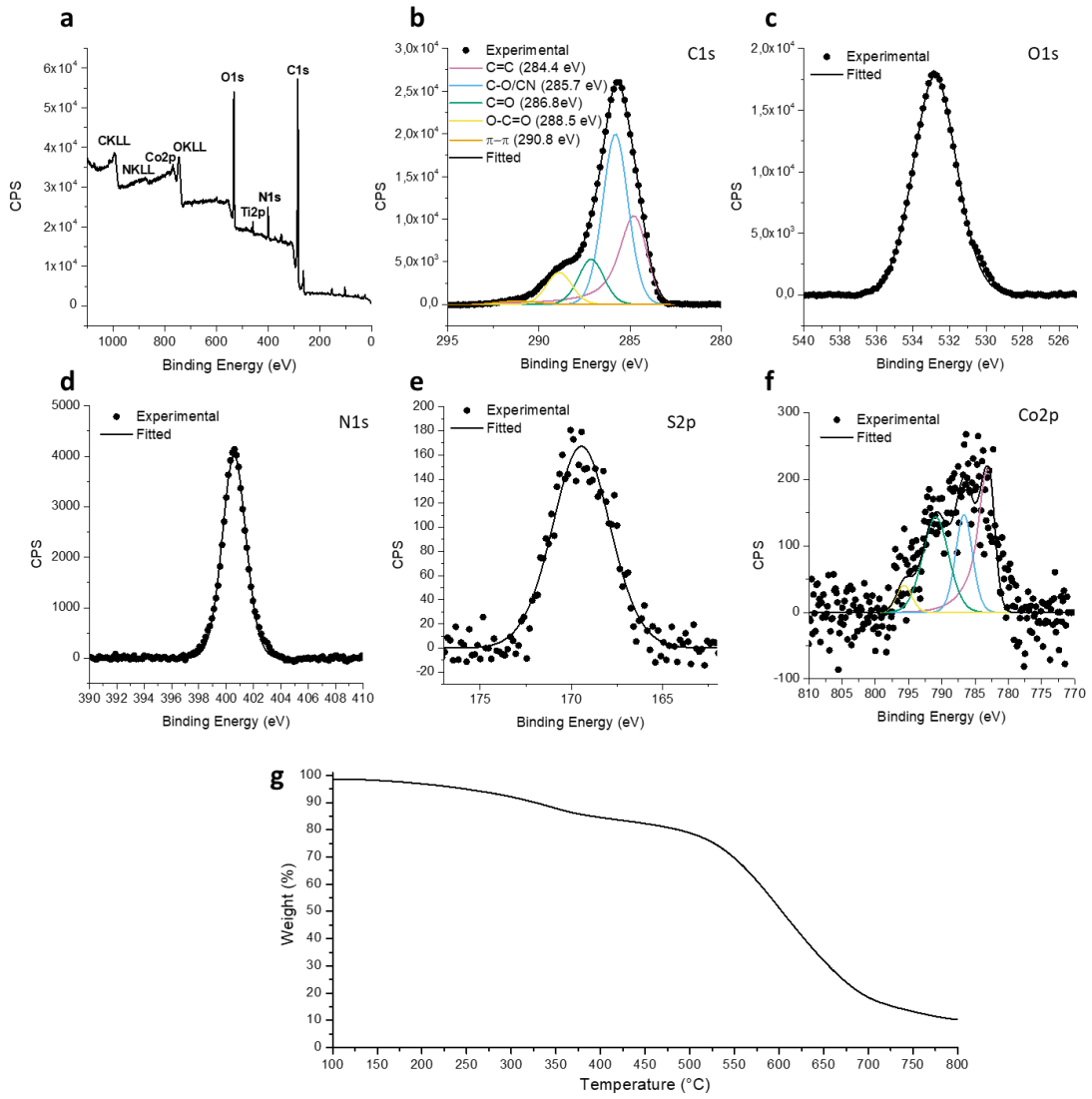

Figure S20. Characterization of EEG-LOx-CoPC. A) Low-resolution XPS survey spectrum. B) High-resolution XPS spectra of the C1s core level. C) High-resolution XPS spectra of the O1s core level. D) High-resolution XPS spectra of the N1s core level. E) High-resolution XPS spectra of the S2p core F) High-resolution XPS spectra of the Co2p core level. G) TGA of EEG-LOx-CoPC under N_2.

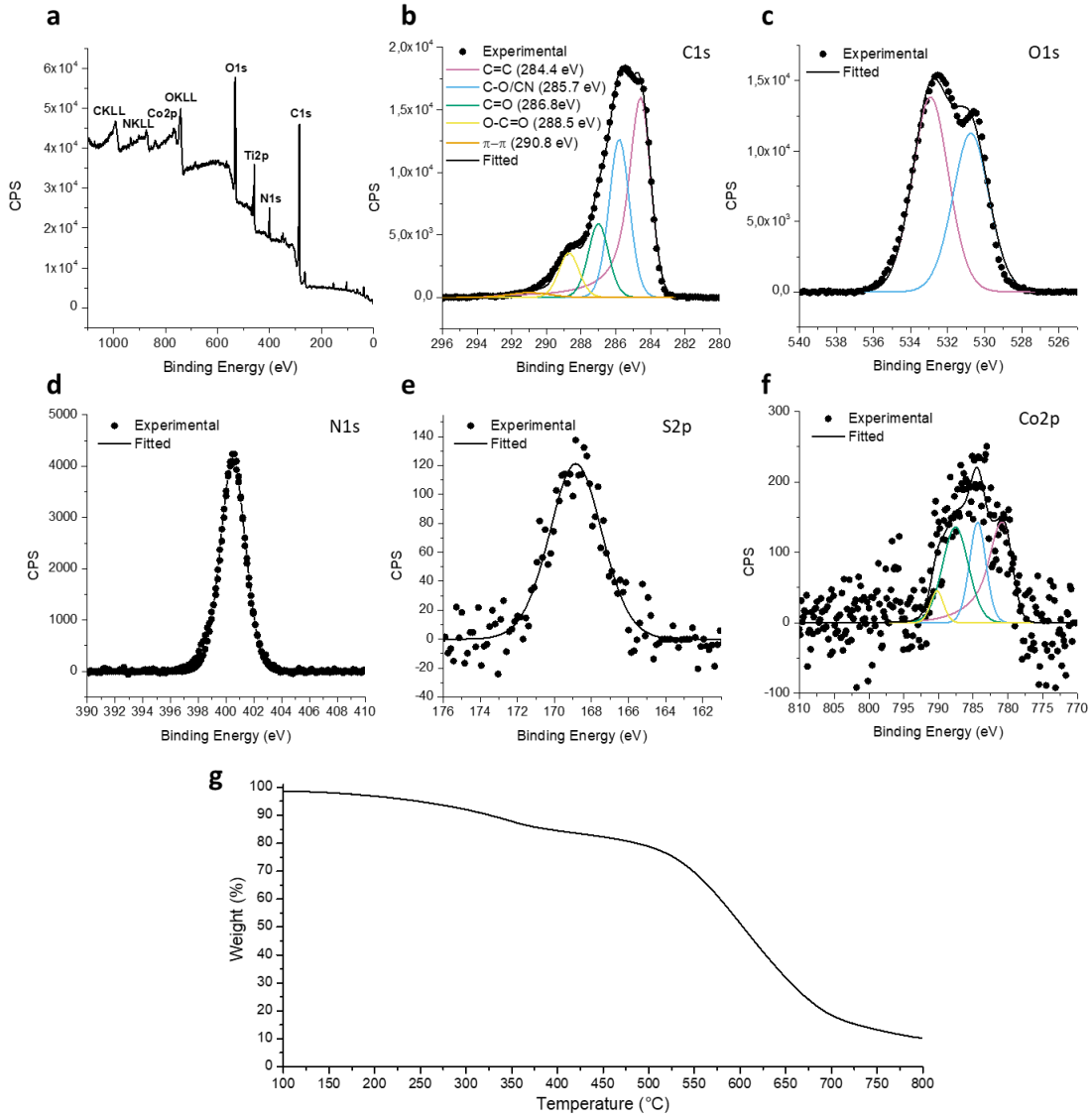

Figure S21. Characterization of EEG-AOx-CoPC. A) Low-resolution XPS survey spectrum. B) High-resolution XPS spectra of the C1s core level. C) High-resolution XPS spectra of the O1s core level. D) High-resolution XPS spectra of the N1s core level. E) High-resolution XPS spectra of the S2p core level. F) High-resolution XPS spectra of the Co2p core level. G) TGA of EEG-AoOx-CoPC under N_2.